

LOW-POWER MEASUREMENT ON A HOM DAMPED CAVITY FOR THE ATF DAMPING RING

S. Sakanaka, F. Hinode, K. Kubo, T. Higo, J. Urakawa and T. Rizawa†
 KEK, National Laboratory for High Energy Physics
 1-1 Oho, Tsukuba-shi, Ibaraki-ken, 305 Japan

† Toshiba Corporation, 2-4 Suchiro-cho, Tsurumi-ku, Yokohama, 230 Japan

Abstract

We describe the results of measurements of HOM (Higher-Order-Mode) characteristics of a low-power test model of the HOM damped cavity for the ATF Damping Ring. Field distributions of observed resonant modes and the loaded-Q's were measured with a bead perturbation technique. Monopole and dipole modes were heavily damped by four damping waveguides with simultaneous use of HOM absorbers on the beam pipe. This cavity almost fulfills the requirement, at least up to the HOM frequency of 2.5 GHz.

Introduction

The ATF (Accelerator Test Facility) Damping Ring [1] is under construction at KEK in order to investigate the production of highly-brilliant multibunch beams required for future linear colliders. High beam current of 600mA that must be supported in the ATF DR requires special design of RF cavities whose HOM impedances are sufficiently lowered.

For this purpose, we designed a 714 MHz HOM damped cavity whose HOMs are strongly damped by four damping waveguides [2]. Two of the waveguides are located at upstream (upper and lower) corners of the cavity while the other two at downstream (left and right) corners. In addition, the simultaneous use of HOM absorbers on thick beam pipes beside the cavity allows us to effectively damp high frequency HOMs (>2.29 GHz for monopole and >1.76 GHz for dipole modes, respectively). Figure 1 shows a cross sectional view of one cavity section equipped with beam-pipe absorbers and tapered transitions. For the absorbing material, some of the SiC's which have the effective conductivity $\sigma_{eff} (= \sigma + \omega\epsilon'')$ of ~100 (Siemens/m) will be used from the trade-off between the microwave absorbing performance and the low-impedance environment for the beam. We used a reaction-bonded SiC ($\sigma_{eff} \sim 200$ S/m at 3 GHz) for the low-power experiments.

The present goal for the cavity HOM impedances are $R (k\Omega) < 2.5/f(\text{GHz})$ for monopole modes, and $R_t (k\Omega/m) < 500$ for dipole modes, where f, R and R_t denote the HOM

frequency, the shunt impedance ($=V^2/P$) and the transverse impedance, respectively.

Low-power Measurements

The performance of HOMs was investigated with a low-power test cavity described in ref. [2]. Figure 1 shows the full structure of the cavity equipped with beam-pipe absorbers. Ends of the damping waveguides were terminated with broadband loads (VSWR < 1.13 for $f > 1$ GHz). Resonant modes were observed by transmission measurements.

In order to assign the modes, we applied a bead perturbation method [3-7]. Using an automated bead-puller and a HP8510B Network Analyzer both under computer control, we measured frequency shifts caused by a small perturbing object (bead) suspended by a thread on the cavity axis. The shift in the resonant frequency is given by [4]

$$\frac{\omega - \omega_0}{\omega_0} = -2\pi r_0^3 (F_1 E_{az}^2 + F_2 E_{at}^2 - \frac{1}{2} F_3 H_{az}^2 - \frac{1}{2} F_4 H_{at}^2) \quad (1)$$

where ω_0 and ω are the unperturbed and the perturbed angular frequencies, respectively, r_0 is half the length of the major axis of the bead, F_1 to F_4 are the form factors, E_a and H_a are proportional to electric and magnetic fields, normalized so that $\int E_a^2 dv = \int H_a^2 dv = 1$, and the subscripts z and t denote the longitudinal and the transverse components, respectively. We measured phase shifts ϕ at unperturbed frequency, and derived the frequency shifts from [5]

$$\frac{\omega - \omega_0}{\omega_0} = \frac{1}{2Q_L} \tan \phi \quad (2)$$

This allows us to measure the frequency shifts even when the loaded-Q (Q_L) is very small, as is noted in ref. [7], by averaging the data over 4096 times. We carried out three sets of the measurements with different metallic objects (sphere, disk and needle), which is sufficient to determine $|E_{az}|$, $|E_{at}|$ and $|H_{at}|$ on the beam axis, except for the TE0-like modes (which have non-zero H_{az} on the cavity axis).

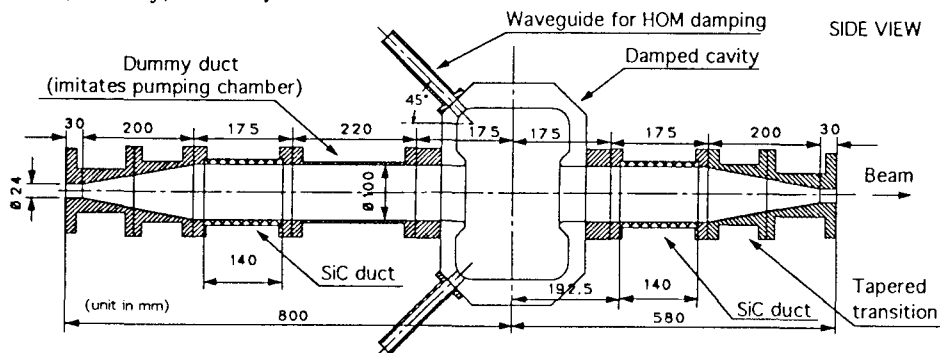
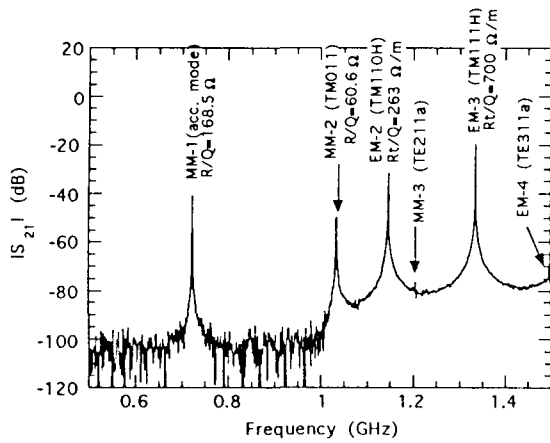
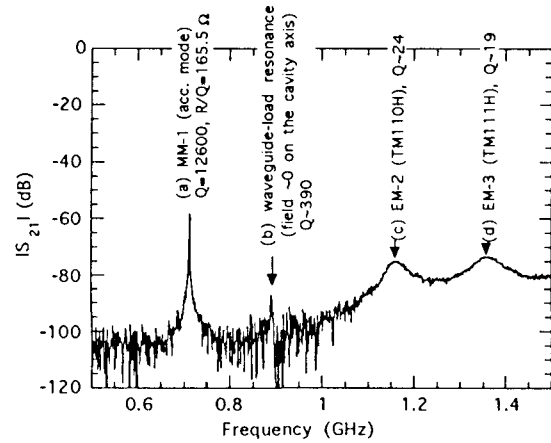


Fig. 1. Cross section of a low-power test cavity equipped with beam-pipe absorbers.



(a) Without damping waveguides. Assigned mode numbers and calculated R/Q or R_l/Q are labeled.



(b) With damping waveguides and loads. Assigned modes and measured loaded- Q 's are labeled.

Fig. 2. Resonance spectra of the test cavity between 0.5 to 1.5 GHz, which were observed by a Network Analyzer.

Before presenting the results, some comments are needed on the classification of modes. In axially symmetric cavities, the resonant modes are classified by the azimuthal index m which represents the angular dependence $\exp(-jm\theta)$ of the fields. In our cavity, however, a quadrupole asymmetry is introduced by the damping waveguides, resulting the resonant modes being the superposition of different angular dependencies. In this case, a simple classification by m (e.g. TM0-EE-1 or 1-EE-1 used in URMEL code) is not sufficient. Instead, we can classify the modes by the boundary conditions (Electric or Magnetic short) on the symmetry planes of $x=0$ and $y=0$. In the rest of this paper, we also use the terms "monopole ($m=0$)" or "dipole ($m=1$)" mode in the sense that they are the lowest order of angular dependencies of the mode.

Results

We observed resonance spectra by measuring the transmission coefficient (S_{21}) between two electric probes put at cavity end-plates, being faced each other in the midplane ($y=0$). With these probes, most of the TM-like modes of interest (monopole, and dipole of one polarization) and some of the TE-like modes could be observed. Figure 2(a) shows the undamped resonance spectrum in the frequency range of 0.5 - 1.5 GHz, with all waveguide ports being sealed on the outer surface of the cavity (but grooves were left at the ports) and with SiC absorbers being exchanged for dummy ducts. The mode numbers assigned from the perturbation method are labeled.

Figure 2(b) shows the damped spectrum with four damping waveguides. The strongest HOMs (TM011-, TM110H- and TM111H- like modes) were heavily damped, which are summarized in Table 1. The measured loaded- Q 's agreed with calculated external- Q 's. Furthermore, the field distributions of TM110H- and TM111H- like modes agreed with the calculated ones (without waveguides). As an example, the field distribution of TM110H-like mode is shown in Fig. 3.

Figure 4(a) shows the undamped HOM spectrum between 1.5 to 2.5 GHz. The azimuthal indices m for the observed

modes were assigned by the same way as described in ref. [6].

Figure 4(b) shows the same frequency range with four damping waveguides. Data with and without the damping by beam-pipe SiC absorbers are shown separately. The measured azimuthal indices m , Q_L 's, and non-zero R/Q 's are also labeled. The HOMs were damped by the waveguides and further by the beam-pipe absorbers. It should be noted that the accurate perturbation measurements were sometimes hard to carry out when there were more than two neighboring resonances being overlapped each other. In such cases, there were some ambiguities in m , Q_L or R/Q for which we put "?" or other comments in Fig. 4(b). Besides, there were other "hidden" resonances which could not be discriminated separately.

TABLE 1. Summary for the Strongest HOMs.

| Mode * | Calculated † | | Calculated‡ | Measured |
|---------------|--------------|----------|------------------|-------------------|
| | f (GHz) | Q_{ex} | R/Q or R_l/Q | f (GHz) Q_L |
| MM-2 (TM011) | 1.075 | 7.1 | 62.5 Ω | not visible |
| EM-2 (TM110H) | 1.160 | 24 | 263 Ω/m | 1.158 24 |
| EM-3 (TM111H) | 1.363 | 24 | 726 Ω/m | 1.363 19 |

† With damping waveguides [2]. ‡ Without damping waveguides.

* H denotes the horizontal deflecting polarization.

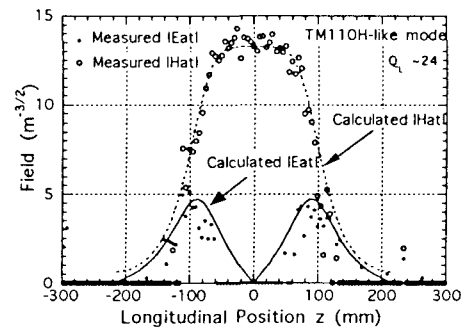


Fig. 3. Measured distribution of transverse electric and magnetic fields of TM110-like mode (with waveguides), together with calculated ones (without waveguides). Note that the distribution was obtained from the phase shifts of less than only 0.25 degrees.

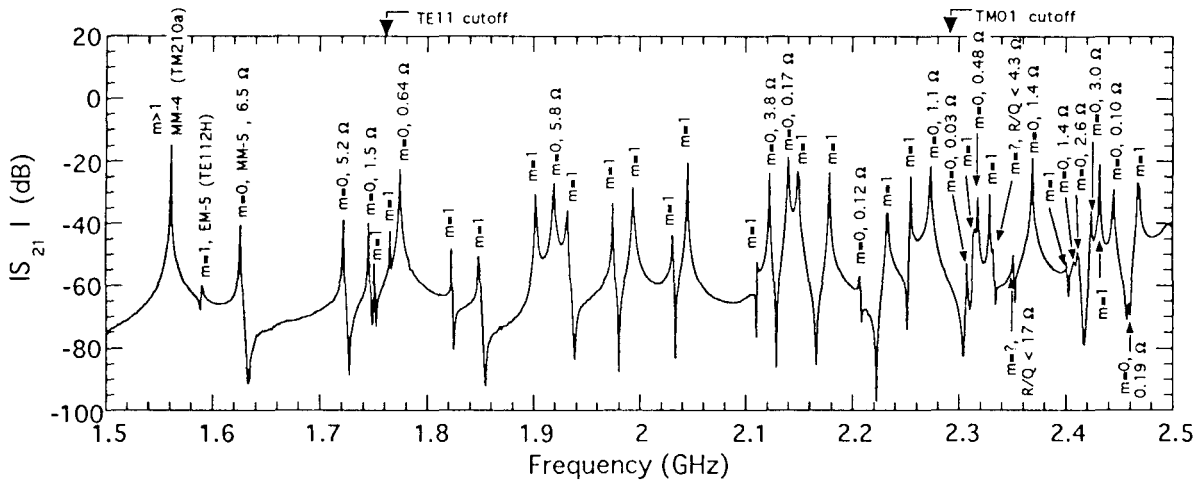


Fig. 4 (a) Undamped HOM spectrum, 1.5 - 2.5 GHz. With no waveguides nor SiC absorbers (which were replaced by dummy ducts). Assigned azimuthal indices m and non-zero R/Q 's from the measurements are labeled.

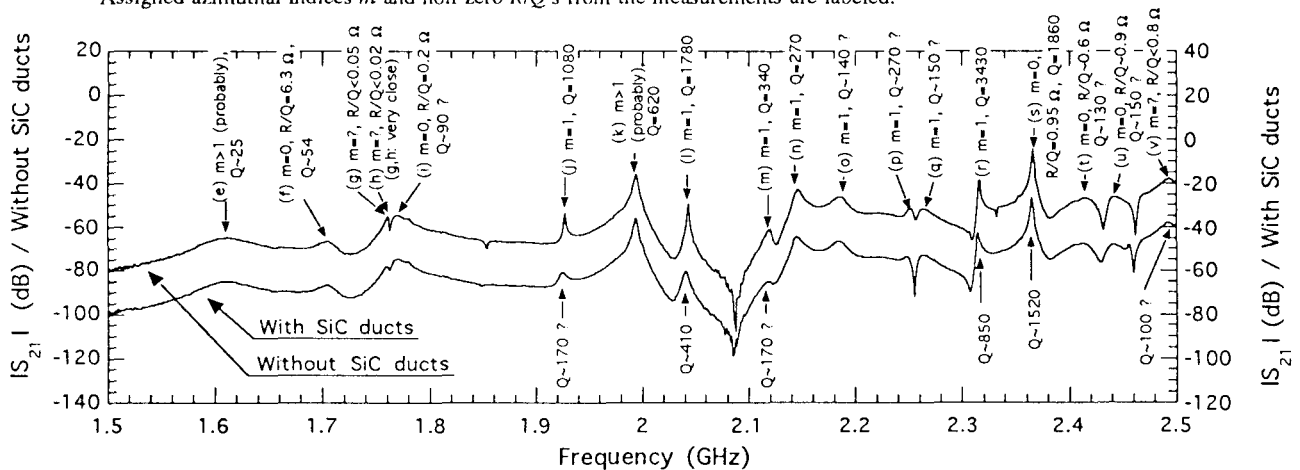


Fig. 4 (b) Damped HOM spectrum with four waveguides, 1.5 - 2.5 GHz. Traces with and without SiC absorbers are shown separately. Assigned azimuthal indices m , Q_L 's, and non-zero R/Q 's from the measurements are labeled.

However, these hidden resonances would be less important because of their low-Q values.

We found that there was no one-to-one correspondence between the damped modes shown in Fig. 4(b) and the undamped modes calculated by 2-dimensional codes (say URMEL) in the high frequency region ($f > 1.5$ GHz). This is due to the mixing of modes caused by the damping waveguides which break the axial symmetry as well as the mirror symmetry with respect to $z=0$ plane.

From Figs. 2(b) and 4(b), the shunt impedances of monopole modes are within the target, except for one mode marked by (s). For this mode, the shunt impedance is 1.4 times larger than the target, which will be cured by additional means. We also obtained good damping performance for the dipole modes. Although (R/Q) 's for the dipole modes in the range of 1.5-2.5 GHz have not yet been calculated, the obtained Q_L 's of lower than 1000 (with SiC ducts) are well within the requirement if their (R/Q) 's are less than 500 Ω/m (which must be so).

Conclusion

Our damped cavity showed excellent damping performance of the monopole and dipole modes, and almost fulfills the requirements at least up to 3.5 times the accelerating frequency. HOM characteristics for higher frequencies will be investigated further. A high-power model is under design towards the test in 1995.

We wish to thank M. Izawa and S. Tokumoto for valuable discussions, and Hajime Nakamura for preparing the computer system used for the measurement.

References

- [1] J. Urakawa et al., *Proc. of XVth International Conference on High Energy Accelerators*, Hamburg, 1992, Vol. I, p. 124.
- [2] S. Sakanaka et al., *Proceedings of the 1993 Particle Accelerator Conference*, Vol. 2, pp. 1027-1029.
- [3] L.C. Maier, Jr. and J.C. Slater, *J. Appl. Phys.* **23** (1952) 68.
- [4] Y. Yamazaki et al., KEK Report 80-8 (1980).
- [5] V. Picciarelli, CERN/EF/RF 82-3 (1982).
- [6] J. Jacob, ESRF-RF/88-02.
- [7] D.A. Goldberg and R.A. Rimmer, *Proceedings of the 1993 Particle Accelerator Conference*, Vol. 2, pp. 871-873.